J Mol Model (2013) 19:4537–4543
DOI 10.1007/s00894-013-1970-1

ORIGINAL PAPER

A new reaction mode of germanium-silicon bond formation: insertion reactions of H_2GeLiF with SiH_3X (X=F, Cl, Br)

Bingfei Yan · Wenzuo Li · Cuiping Xiao · Qingzhong Li · Jianbo Cheng

Received: 16 June 2013 / Accepted: 31 July 2013 / Published online: 16 August 2013

Abstract A combined density functional and *ab initio* quantum chemical study of the insertion reactions of the germylenoid H_2GeLiF with SiH_3X (X=F, Cl, Br) was carried out. The geometries of all the stationary points of the reactions were optimized using the DFT B3LYP method and then the QCISD method was used to calculate the single-point energies. The theoretical calculations indicated that along the potential energy surface, there were one precursor complex (Q), one transition state (TS), and one intermediate (IM) which connected the reactants and the products. The calculated barrier heights relative to the respective precursors are 102.26 (X=F), 95.28 (X=Cl), and 84.42 (X=Br) kJ mol^{-1} for the three different insertion reactions, respectively, indicating the insertion reactions should occur easily according to the following order: SiH_3-Br>SiH_3-Cl>SiH_3-F under the same situation. The solvent effects on the insertion reactions were also calculated and it was found that the larger the dielectric constant, the easier the insertion reactions. The elucidations of the mechanism of these insertion reactions provided a new reaction model of germanium-silicon bond formation.

Keywords B3LYP · H_2GeLiF · Insertion reaction · QCISD · SiH_3X (X=F, Cl, Br)

Introduction

The research of germanium compounds and their reactions is an interesting topic since many organic germanium compounds have been found to have biologic activities [1–4]. The theoretical study and complementary experiments of germanium compounds have made dramatic advances over the past few years [5–15].

Germylenoid R_1R_2GeMX (M=alkali metal, X=halogen) is one of the derivatives of germylene. As analogous to carbenoid R_1R_2CMX [16, 17] and silylenoid R_1R_2SiMX [18, 19], germylenoid may be more stable than germylene R_1R_2Ge and has some particular reactive properties. In 1991, Gaspar et al. [20] firstly suggested that germylenoid might be the intermediate involved in the reaction of dichlorodimethylgermane with substituted butadiene in THF solvent. In 2000, Ichinohe et al. [21] pointed out that in the reaction of $GeCl_2$·dioxane with $^tBu_3SiNa$, one germylenoid $^tBu_3SiGeCl_2Na$ was a reactive intermediate. In 2005, Tajima et al. [10] synthesized extremely hindered bis(germacyclopropa)benzenes. The authors [10] considered that the formation of bis(germacyclopropa)benzenes should be interpreted in terms of the concurrent generation of different reactive species such as the intermediate germylenoid Tbt(Dip)GeBrLi and benzyne species in the reaction under the mild conditions. In 2006, Sasamori et al. [22] described the initial work on the sila- and germacyclopropabenzenes. They thought that germylenoid Tbt(Dip)GeLiBr was an important intermediate in the addition reaction. Very recently, Filippou et al. [23] synthesized some compounds containing metal-germanium triple bonds and in this work the germylenoid should be an important reactant. However, no stable germylenoid has been synthesized successfully till now. Therefore, it is necessary to carry out systemic theoretical study on germylenoids to investigate their structures, properties, and reactions.

There were some theoretical works on germylenoid. In 1999, Qiu et al. [24] firstly examined the isomeric structure of the simplest germylenoid H_2GeLiF by *ab initio* calculations. Until now, a few kinds of germylenoids have been investigated such as H_2GeLiX [24–27], H_2GeNaF [28], $H_2GeClMgCl$ [29], $H_2GeClAlCl_2$ [30], $H_2GeClBeCl$ [31], HB=GeLiF [32], H_2C=GeNaF [33], and HN=GeNaF [34]. As aforementioned, germylenoid was active intermediate and

B. Yan · W. Li (✉) · C. Xiao · Q. Li · J. Cheng
The Laboratory of Theoretical and Computational Chemistry, School of Chemistry and Chemical Engineering, Yantai University, Yantai 264005, People's Republic of China
e-mail: liwenzuo2004@126.com

played important roles in many organic reactions [20–23]. If people understand the reactivity of germylenoid correctly, the proper methods would be carried out to synthesize new germanium-containing compounds using germylenoid. Therefore it is necessary to study the reactions of the germylenoid with other substances systemically. To our best knowledge, theoretical studies on the reactions of germylenoids were not many and only some reactions of germylenoids with small molecules, such as HF, H_2O, NH_3, CH_4, and CH_3X (X=F, Cl, Br) [27, 28, 32, 34–37] have been calculated. However, the insertion reactions of germylenoid into Si-X bonds have not been reported. In order to fill this gap and extend the reactions of the germylenoid, we have investigated the insertion reactions of the germylenoid H_2GeLiF with SiH_3X (X=F, Cl, Br) using the density functional and *ab initio* quantum chemical calculations recently. Through this theoretical work, we hope (i) to optimize the structures of all stationary points, (ii) to determine the thermodynamics of the insertion reactions, (iii) to predict their activation barriers, (iv) to elucidate the reaction mechanisms, and (v) to evaluate the solvent effects on the insertion reactions of H_2GeLiF with SiH_3X (X=F, Cl, Br). The elucidations of the mechanism of these insertion reactions would provide a new reaction model of germanium-silicon bond formation.

Computational methods

The computational details were described elsewhere [36]. The geometries for the stationary points were computed with the Gaussian 09 program suits [38]. The DFT (density functional theory) B3LYP (Becke's three-parameter hybrid function with the non-local correlation of Lee–Yang–Parr) [39, 40] method with the 6-311+G (d, p) [41] basis set were used for all computations. All geometries were first optimized and then the harmonic vibrational frequencies were calculated at the same level to confirm the properties of the stationary points. The insertion reaction pathways for the mechanism discussed were verified using intrinsic reaction coordinate (IRC) [42] analyses for all TS structures to verify the reactants and the products to which each TS was connected. The electrostatic potential computations were carried out on the optimum geometries at the B3LYP/6-311+G (d, p). In order to improve the treatment of electron correlation, the single-point calculations were performed at the QCISD [43, 44] level using the 6-311++G(d, p) basis set for all atoms. Unless otherwise noted, the relative energies given in the present paper were those determined at QCISD/6-311++G(d, p)//B3LYP/6-311+G (d, p) and included zero-point vibrational energy (ZPE, without scale) corrections determined at B3LYP/6-311+G (d, p) level. To consider solvent effects on the insertion reactions, the PCM (polarized continuum model) [45–47] was applied to the calculations. The solvents cyclohexane (C_6H_{12}, dielectric constant ε=2.016), tetrahydrofuran (THF, ε=7.426), acetone (CH_3COCH_3, ε=20.493), methyl alcohol (CH_3OH, ε=32.613), dimethyl sulfoxide (DMSO, ε=46.826), and water (H_2O, ε=78.355) were used.

Results and discussion

The previous calculations [24, 27] show that germylenoid H_2GeLiF had three equilibrium configurations, in which the *p*-complex structure had the lowest energy and was the most stable structure. Consequently, the *p*-complex structure of H_2GeLiF was selected as the reactant when we analyzed the insertion reactions of germylenoid H_2GeLiF with SiH_3X (X=F, Cl, Br).

As shown in Fig. 1, the *p*-complex germylenoid H_2GeLiF can be regarded as a singlet complex in which electrons of the F atom in LiF are donated into the empty *p*-orbital of Ge atom in H_2Ge. The electrostatic potential computations indicate that in SiH_3X there is more negative charge lying on the halogen atom X and positive charge lying on the silicon atom. When SiH_3X approaches germylenoid H_2GeLiF with the halogen atom X and SiH_3 attacking the unoccupied *p*-orbital and the σ lone-pair electrons of Ge atom respectively, insertion reactions take place.

The insertion reactions of germylenoid H_2GeLiF with SiH_3X (X=F, Cl, Br) could be described as the following formula:

$$H_2GeLiF + SiH_3X \rightarrow H_2XGe{-}SiH_3 + LiF \ (X = F, Cl, Br)$$

Based on the calculated results, we found that there are one precursor complex (Q), one transition state (TS), and one intermediate (IM) which connected the reactants and the products along the potential energy surface. The geometries of reactants, Qs, TSs, IMs, and products are shown in Fig. 2.

The structures and energies of the precursor complexes

When halogenated silane SiH_3X approaches germylenoid H_2GeLiF, the initial formation of the precursor complexes Q1, Q2, and Q3 are facilitated by the interaction between the

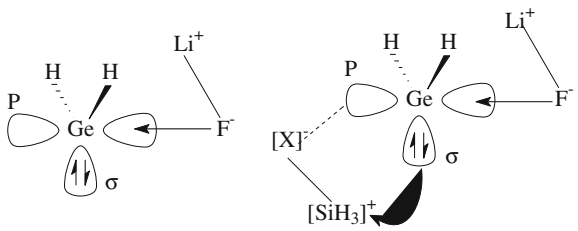

Fig. 1 The *p*-complex H_2GeLiF and its insertion reaction paths with SiH_3X (X=F, Cl, Br)

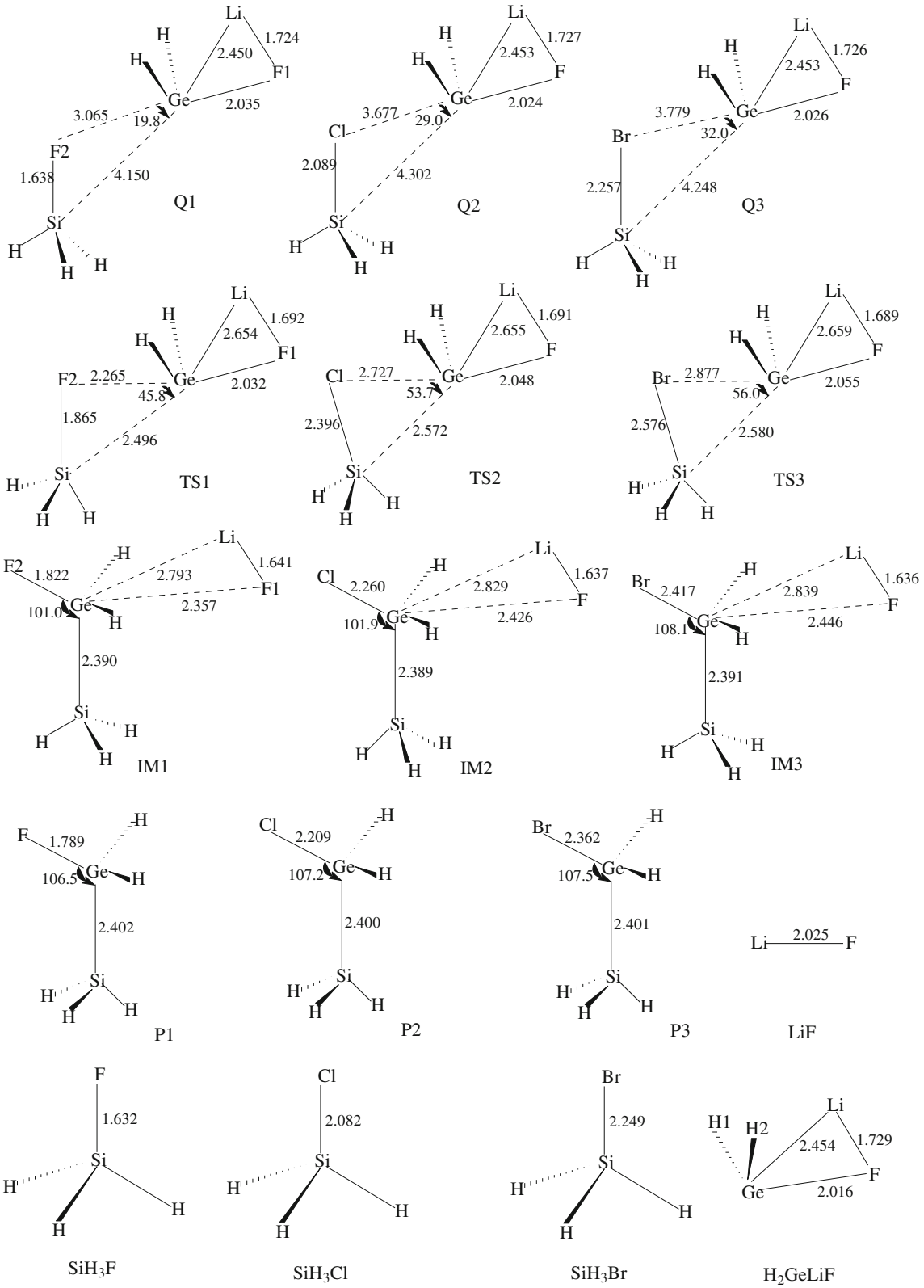

Fig. 2 The geometries of the stationary points of the insertion reactions of the germylenoid H_2GeLiF with SiH_3X (X=F, Cl, Br) in gas phase calculated at B3LYP/6-311+G (*d*, *p*) level (Bond lengths are given in angstroms and angles in degrees)

p-orbital on Ge atom and the negative X atom of SiH_3X. The precursor complexes adopt C_1 symmetry and involve inversion of configuration. Compared with the separated structures of SiH_3X and H_2GeLiF molecules, the moieties of

SiH_3X and H_2GeLiF in Q1, Q2, and Q3 change very little, respectively. From Fig. 2, it can be seen that the Ge-X (X=F, Cl, Br) bond lengths in Q1, Q2, and Q3 are very long, and the Si-X bonds are found to be slightly longer than their corresponding Si-X bond lengths in the isolated reactants SiH_3X. The energies of the precursor complexes Q1, Q2, and Q3 are lower than their corresponding reactants by 7.23, 8.49, and 8.47 kJ mol^{-1}, respectively (Table 1). The long Ge-X bond lengths, the slight elongation of Si-X bond lengths, and the small relative energies of the precursor complexes (Q1, Q2, and Q3) indicate that the interaction of Ge atom and X atom is very weak.

The structures and energies of the transition states

Based on the electrostatic potential computations, we found that there is a positive σ hole on Si. When SiH_3 gradually approaches the σ lone-pair electrons of Ge atom, the TSs create. As displayed in Fig. 2, the calculated transition states TS1, TS2, and TS3 in the insertion reactions have the similar structures. There is a three-membered-ring structure (Si-Ge-X, X=F, Cl, Br) in each TS. The Si–X bond broken in TSs are lengthened by 0.233 (X=F), 0.314 (X=Cl), 0.327 Å (X=Br), compared to the isolated SiH_3X, where the bond elongation correspond to about 14.3, 15.1, and 14.5 % of its original length, respectively. These reveal that the migrating halogen atom X has a strong reactant-like character. On the other hand, the Ge-X bonds forming in TSs are found to be greatly shorter than their corresponding Ge-X bond lengths in the Qs. The bond angles X-Ge-Si increase from Qs toward TSs, by 26.0, 24.7, and 24.0°, respectively. According to the Hammond's postulate [48], the three transition states are all early TSs.

The frequency analysis calculations are made at the B3LYP/6-311+G (d, p) level. The calculations indicate that all TSs have unique imaginary frequency, which are 130.0i, 245.6i, and 209.4i cm^{-1}, respectively. The unique imaginary frequency vibration involves bond formation between Ge and Si in concert with Si-X bond breaking, and X migration to Ge. The IRC calculations displayed that the transition states connected the precursor complexes and the intermediates. As listed in Table 1, the relative energies of TS1, TS2, and TS3 to their reactants are 95.03, 86.79, and 75.95 kJ mol^{-1}, respectively. Therefore, the reaction barriers relative to the respective precursors are 102.26 (X=F), 95.28 (X=Cl), and 84.42 kJ mol^{-1} (X=Br), respectively.

The structures and energies of the intermediates and products

As shown in Fig. 2, three intermediates of the three insertion reactions have similar bipyramid structures formed between Ge atom and its adjacent atoms. The bond angles X-Ge-Si (X=F, Cl, Br) increase dramatically from TSs toward IMs, by 55.2, 48.2, and 46.3°, respectively. In the IMs, the Si–X bonds have been broken completely. The Ge–Si and Ge–X (X=F, Cl, Br) bond lengths of IMs are shorter than those of TSs respectively. The Ge-Si bond lengths of IMs are 0.106, 0.183, 0.189 Å shorter than those of TSs and Ge-X (X=F, Cl, Br) bond lengths obviously decrease from TSs toward IMs, by 0.443, 0.467, and 0.460 Å. The shortening of the Ge–Si and Ge–X (X=F, Cl, Br) bond lengths indicate that the Ge–Si and Ge–X (X=F, Cl, Br) bond have been almost formed. As listed in Table 1, the relative energies of IM1, IM2, and IM3 to their reactants are −2.16, –56.55, and −64.68 kJ mol^{-1}, respectively.

After getting over the transition states, the IMs can further decompose to substituted germane $H_2XGe\text{-}SiH_3$ and LiF, which are the products of the insertion reactions of H_2GeLiF and SiH_3X (X=F, Cl, Br). The LiF moiety leaving from Ge atom is monotonously energy increasing process. The sum of the energies of $H_2XGe\text{-}SiH_3$ and LiF are above the energies of IMs by 62.54, 52.92, 50.40 kJ mol^{-1}, respectively. Compared with the reactants, the relative energies of the final products ($H_2XGe\text{-}SiH_3$+LiF) are 60.38 (X=F), -3.63 (X=Cl), and −14.28 kJ mol^{-1} (X=Br), respectively.

The mechanisms of the insertion reactions

Here we choose the insertion reaction of H_2GeLiF with SiH_3Cl as an example. IRC calculations have been performed

Table 1 Relative energies[a] (in kJ mol^{-1}) of precursor complexes (Qs), transition states (TSs), intermediates (IMs), and products in solvents

Solvents	Q1	TS1	IM1	P1+LiF	Q2	TS2	IM2	P2+LiF	Q3	TS3	IM3	P3+LiF
Gas phase	−7.23	95.03	−2.16	60.36	−8.49	86.79	−56.55	−3.63	−8.47	75.95	−64.68	−14.28
C_6H_{12}	−7.45	73.31	−19.98	28.50	−8.97	66.97	−74.51	−35.86	−8.78	57.28	−82.49	−45.75
THF	−6.20	56.75	−30.78	3.11	−8.20	52.49	−85.02	−60.62	−7.90	43.42	−92.72	−70.29
Acetone	−5.79	52.34	−33.73	−2.96	−7.90	48.60	−87.95	−66.53	−7.57	39.64	−95.57	−76.14
Methanol	−5.69	51.39	−34.36	−4.22	−7.82	47.76	−88.59	−67.75	−7.50	38.82	−96.20	−77.35
DMSO	−5.63	50.90	−34.70	−4.86	−7.78	47.33	−88.92	−68.38	−7.45	38.39	−96.52	−77.97
H_2O	−5.58	50.45	−35.00	−5.44	−7.74	46.93	−89.23	−68.95	−7.41	38.00	−96.83	−78.54

[a] Calculated at the QCISD/6-311++G(*d*, *p*)//B3LYP/6-311+G(*d*, *p*) level

on the basis of the optimized TS2 to investigate the interaction between H_2GeLiF and SiH_3X in the insertion process. The total energy changes and the variations of Ge-F, Ge-Cl, Ge-Si, and Si-Cl bond distances along the IRC path are shown in Fig. 3. From Fig. 3, it can be seen that as the reaction coordinate passes from point −5.0 to 0.0, the total energy increases sharply and reaches its maximum at point 0.0. In this region, the lengths of Ge-F and Si-Cl bond increase and the lengths of Ge-Si and Ge-Cl bond decrease obviously. As for the Si-Cl and Ge-Cl bond distances, they increase and decrease with the proceeding of the reaction, implying the break of the former and the formation of the latter, respectively. We think the insertion reactions of H_2GeLiF with SiH_3X (X=F, Br) have a similar mechanism with $H_2GeLiF+SiH_3Cl$ reaction.

The comparisons of three insertion reactions

The calculated barrier heights relative to the respective precursors are 102.26 (X=F), 95.28 (X=Cl), and 84.42 (X=Br) kJ mol^{-1} for the three different insertion reactions, respectively, revealing their different reactivities. Consequently, the calculated relative reaction free energies of them are 60.38 (X=F), -3.63 (X=Cl), -14.28 kJ mol^{-1} (X=Br), respectively. Consequently, from the thermodynamic and kinetic viewpoints, the insertion reactions H_2GeLiF plus SiH_3X should occur easily according to the following order: SiH_3-Br>SiH_3-Cl>SiH_3-F under the same situation. This order can be explained by comparing the Si-X bond energies. For Si-F, Si-Cl, and Si-Br, the bond energies are 565, 381, and 310 [49] kJ mol^{-1}, respectively. Therefore, amomg the three reactions, the $H_2GeLiF+SiH_3F$ is the most difficult to react, the reaction of H_2GeLiF with SiH_3Cl is much easier than with SiH_3F, and the reaction of $H_2GeLiF+SiH_3Br$ is the easiest.

The solvent effect

To consider the solvent effects on these reactions, using the PCM model and the C_6H_{12}, THF, acetone, methyl alcohol, DMSO, and H_2O solvents, the QCISD/6-311++G(d, p) single-point calculations were performed at the B3LYP/6-311+G (d, p) optimized geometries. The relative energies of all stationary points calculated in various solvents are also listed in Table 1. It can be seen from Table 1 that the relative energies of the TSs, IMs, and products for the three insertion reactions calculated in various solvents are lower respectively than those calculated in gas phase. Compared with those in gas phase, the barrier heights in various solvents are lower, implying insertion reactions of H_2GeLiF with SiH_3X are easier to occur in solvents. On the other hand, it can be seen from Table 1, with the raising of dielectric constant, the insertion reactions occur more easily. Therefore, the insertion reactions of H_2GeLiF with SiH_3X occur easily according to the following order: H_2O>DMSO>methyl alcohol>acetone >THF>C_6H_{12}>gas phase.

Comparisons of the insertion reactions of H_2GeLiF with SiH_3X and CH_3X (X=F, Cl, Br)

We [37] have studied the insertion reactions of H_2GeLiF with CH_3X (X=F, Cl, Br) using the DFT B3LYP and QCISD methods. By comparing with the present work and reference [37], we can find some facts as follows: (a) the mechanisms of the two kinds of insertion reactions are identical; (b) The reaction barriers of the insertion reactions of H_2GeLiF with SiH_3X are lower than those with CH_3X, respectively, indicating that the insertion reactions of H_2GeLiF with YH_3X (Y=C, Si) occur easily according to the following order: SiH_3X> CH_3X under the same situation. For example, when X=Cl, the

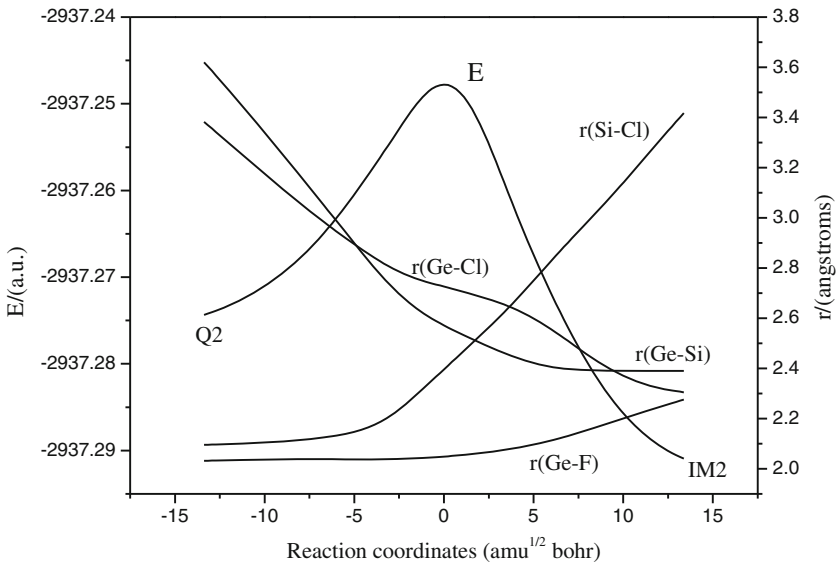

Fig. 3 The changes of energies and bond distances along the reaction coordinates of the reaction of $H_2GeLiF+SiH_3Cl$

reaction barrier of the insertion reaction of H_2GeLiF with SiH_3Cl is 95.28 kJ mol^{-1}, while the reaction barrier of the insertion reaction of H_2GeLiF with CH_3Cl is 238.01 kJ mol^{-1} [37]. Obviously, under the same situation, the reaction of $H_2GeLiF+SiH_3Cl$ occurs easier than $H_2GeLiF+CH_3Cl$; (c) For both kinds of reactions, the solvent effects are similar: in solvents, the insertion reactions occur easier than in vacuum.

Conclusions

In this work, we studied the insertion reactions of the germylenoid H_2GeLiF with SiH_3X (X=F, Cl, Br) for the first time by using the DFT B3LYP and QCISD methods. The theoretical calculations indicated that along the potential energy surface, there were one precursor complex (Q), one transition state (TS), and one intermediate (IM) which connected the reactants and the products. The reactions proceeded through a three-member-ring transition state structure, involving the Ge atom, the Si atom, and the migrating halogen X atom. The three reactions generally followed a similar reactivity pattern. From the thermodynamic and kinetic viewpoints, the calculated results indicated that under the same condition the insertion reactions should occur easily according to the following order: SiH_3-Br>SiH_3-Cl>SiH_3-F. The solvent effects on the insertion reactions were also calculated and it was found that the larger the dielectric constant, the easier the insertion reactions.

Acknowledgments This research was supported by the National Natural Science Foundation Committee of China (No. 21103145), the Natural Science Foundation of Shandong Province (No.ZR2009BQ006), the Fund for Doctor of Yantai University (No. HY05B30), and the Special Foundation of Youth Academic Backbone of Yantai University. Professor Cheng acknowledges support by the Open fund (sklssm201216) of the State Key Laboratory of Supramolecular Structure and Materials, Jilin University.

References

1. Evans DA, Woerpel KA, Faul MM (1991) J Am Chem Soc 113:726–728
2. Nishiyama H, Itoh Y, Matsumoto H, Park SB, Itoh K (1994) J Am Chem Soc 116:2223–2224
3. Riviere B, Monique D (2000) J Organomet Chem 595:153–157
4. Kassaee MZ, Ghambarian M, Musavi SM (2005) J Organomet Chem 690:4692–4703
5. Sekiguchi A, Lee VY (2003) Chem Rev 103:1429–1448
6. Huo Y, Berry DH (2005) Chem Mater 17:157–163
7. Xi HW, Lim KH (2008) Organometallics 27:5748–5758
8. Ferro L, Hitchcock PB, Coles MP, Fulton JB (2012) Inorg Chem 51:1544–1551
9. Konno Y, Kudo T, Sakai S (2011) Theor Chem Acc 130:371–383
10. Sasamori T, Tokitoh N (2006) Organometallics 25:3522–3532
11. Broeckaert L, Geerlings P, Růžička A, Willem R, De Proft F (2012) Organometallics 31:1605–1617
12. West JK, Stahl L (2012) Organometallics 31:2042–2052
13. Brown ZD, Guo J-D, Nagase S, Power PP (2012) Organometallics 31:3768–3772
14. Novotný M, Padělková Z, Holeček J, Růžička A (2013) J Organomet Chem 733:71–78
15. Menchikov LG, Ignatenko MA (2013) Pharmaceutical Chem J 46:635–638
16. Boche G, Lohrenz JCW (2001) Chem Rev 101:697–756
17. Capriati V, Florio S (2010) Chem Eur J 16:4152–4162
18. Flock M, Marschner C (2005) Chem Eur J 11:4635–4642
19. Molev G, Bravo-Zhivotoskii D, Karni M, Tumanskii B, Botoshansky M, Apeloig Y (2006) J Am Chem Soc 128:2784–2785
20. Lei DQ, Gaspar PP (1991) Polyhedron 10:1221–1225
21. Ichinohe M, Sekiyama H, Fukaya N, Sekiguchi A (2000) J Am Chem Soc 122:6781–6782
22. Tajima T, Sasamori T, Takeda N, Tokitoh N, Yoshida K, Nakahara M (2006) Organometallics 25:230–235
23. Filippou AC, Stumpf KW, Chernov O, Schnakenburg G (2012) Organometallics 31:748–755
24. Qiu HY, Ma WY, Li GB, Deng CH (1999) Chinese Chem Lett 10:511–514
25. Zhu YF, Fang YZ, Zhou JH, Ma WY (2007) Chinese J Struct Chem 26:395–400
26. Ma WY, Zhu YF, Zhou JH, Fang YZ (2007) J Mol Struct (Theochem) 817:77–81
27. Tan X, Li P, Wang D, Yang X (2006) J Mol Struct (Theochem) 761:27–30
28. Tan X, Li P, Yang X, Wang D (2006) Int J Quan Chem 106:1902–1906
29. Li WZ, Cheng JB, Li QZ, Gong BA, Sun JZ (2009) Acta Phys-Chim Sin 25:121–125
30. Li WZ, Cheng JB, Li QZ, Gong BA, Sun JZ (2009) J Organomet Chem 694:2898–2901
31. Li WZ, Gong BA, Cheng JB, Xiao CP (2007) J Mol Struct (Theochem) 847:75–78
32. Li WZ, Yang FX, Cheng JB, Li QZ, Gong BA (2012) Chinese J Struct Chem 31:19–26
33. Li WZ, Cheng JB, Gong BA, Xiao CP (2006) J Organomet Chem 691:5984–5987
34. Tan X, Wang W, Li P, Wang Q, Zheng G, Liu F (2008) J Organomet Chem 693:475–482
35. Tan X, Wang W, Li P, Liu F (2009) Russian J Phys Chem A 83:1355–1362
36. Li WZ, Liu T, Cheng JB, Li QZ, Gong BA, Sun JZ (2010) J Organomet Chem 695:909–912
37. Li WZ, Yan BF, Li QZ, Cheng JB (2013) J Organomet Chem 724:163–166
38. Frisch MJ, Trucks GW, Schlegel HB, Scuseria GE, Robb MA, Cheeseman JR, Montgomery JA Jr, Vreven T, Kudin KN, Burant JC, Millam JM, Iyengar SS, Tomasi J, Barone V, Mennucci B, Cossi M, Scalmani G, Rega N, Petersson GA, Nakatsuji H, Hada M, Ehara M, Toyota K, Fukuda R, Hasegawa J, Ishida M, Nakajima T, Honda Y, Kitao O, Nakai H, Klene M, Li X, Knox JE, Hratchian HP, Cross JB, Adamo C, Jaramillo J, Gomperts R, Stratmann RE, Yazyev O, Austin AJ, Cammi R, Pomelli C, Ochterski JW, Ayala PY, Morokuma K, Voth GA, Salvador P, Dannenberg JJ, ZakrzewskiVG DS, Daniels AD, Strain MC, Farkas O, Malick DK, Rabuck AD, Raghavachari K, Foresman JB, Ortiz JV, Cui Q, Baboul AG, Clifford S, Cioslowski J, Stefanov BB, Liu G, Liashenko A, Piskorz P, Komaromi I, Martin RL, Fox DJ, Keith T, Al-Laham MA, Peng CY, Nanayakkara A, Challacombe M, Gill PMW, Johnson B, Chen W, Wong MW, Gonzalez C, Pittsburgh PA, Pople JA (2009) Gaussian 09, Revision A02. Gaussian Inc, Wallingford
39. Becke AD (1993) J Chem Phys 98:5648–5652
40. Lee C, Yang W, Parr RG (1988) Phys Rev B 37:785–789

41. Hehre WJ, Radom L, Schleyer PVR, Pople JA (1986) Wiley, New York
42. Gonzales C, Schlegel HB (1991) J Chem Phys 95:5853–5860
43. Gauss J, Cremer C (1988) Chem Phys Lett 150:280–286
44. Salter EA, Trucks GW, Bartlett RJ (1989) J Chem Phys 90:1752–1766
45. Mennucci B, Tomasi J (1997) J Chem Phys 106:5151–5158
46. Cancès MT, Mennucci B, Tomasi J (1997) J Chem Phys 107:3032–3041
47. Cossi M, Barone V, Mennucci B, Tomasi J (1998) Chem Phys Lett 286:253–260
48. Hammond GS (1955) J Am Chem Soc 77:334–338
49. http://www.wiredchemist.com/chemistry/data/bond_energies_lengths.html.